Journal of Physiology (2002), **545.2**, *pp.* 453–461
DOI: 10.1113/jphysiol.2002.025866

www.jphysiol.org

Stoichiometry of Na^+–Ca^{2+} exchange is 3:1 in guinea-pig ventricular myocytes

Masamitsu Hinata, Hisao Yamamura *, Libing Li, Yasuhide Watanabe †, Tomokazu Watano, Yuji Imaizumi * and Junko Kimura

*Department of Pharmacology, School of Medicine and †Department of Ecology and Clinical Therapeutics, School of Nursing, Fukushima Medical University, Fukushima 960-1295 and * Department of Molecular and Cellular Pharmacology, Graduate School of Pharmaceutical Sciences, Nagoya City University, Nagoya 467-8603, Japan*

In single guinea-pig ventricular myocytes, we examined the stoichiometry of Na^+–Ca^{2+} exchange (NCX) by measuring the reversal potential (E_{NCX}) of NCX current (I_{NCX}) and intracellular Ca^{2+} concentration ($[Ca^{2+}]_i$) with the whole-cell voltage-clamp technique and confocal microscopy, respectively. With given ionic concentrations in the external and pipette solutions, the predicted E_{NCX} were −73 and −11 mV at 3:1 and 4:1 stoichiometries, respectively. E_{NCX} measured were −69 ± 2 mV (n = 11), −47 ± 1 mV (n = 14) and −15 ± 1 mV (n = 15) at holding potentials (HP) of −73, −42 and −11 mV, respectively. Thus, E_{NCX} almost coincided with HP, indicating that $[Ca^{2+}]_i$ and/or $[Na^+]_i$ changed due to I_{NCX} flow. Shifts of E_{NCX} (ΔE_{NCX}) were measured by changing $[Ca^{2+}]_o$ or $[Na^+]_o$. The measured values of ΔE_{NCX} were almost always smaller than those expected theoretically at a stoichiometry of either 3:1 or 4:1. Using indo-1 fluorescence, $[Ca^{2+}]_i$ measured under the whole-cell voltage-clamp supported a 3:1 but not 4:1 stoichiometry. To prevent Ca^{2+} accumulation, we inhibited I_{NCX} with Ni^{2+} and re-examined E_{NCX} during washing out Ni^{2+}. With HP at predicted E_{NCX} at a 3:1 stoichiometry, E_{NCX} developed was close to predicted E_{NCX} and did not change with time. However, with HP at predicted E_{NCX} for a 4:1 stoichiometry, E_{NCX} developed initially near a predicted E_{NCX} for a 3:1 stoichiometry and shifted toward E_{NCX} for a 4:1 stoichiometry with time. We conclude that the stoichiometry of cardiac NCX is 3:1.

(Received 6 June 2002; accepted after revision 25 September 2002; first published online 1 November 2002)
Corresponding author M. Hinata: Department of Pharmacology, School of Medicine, Fukushima Medical University, Fukushima 960-1295, Japan. Email: mhinata@fmu.ac.jp

Na^+–Ca^{2+} exchange (NCX) is a key regulator of intracellular Ca^{2+} in cardiac myocytes. Ca^{2+} is extruded in exchange with Na^+ reversibly. Transport of Na^+ and Ca^{2+} via NCX is sequential, not simultaneous (Kananshvili, 1990; Li & Kimura, 1991; Niggli & Lederer, 1991). The energy for transport depends on the Na^+ and Ca^{2+} concentration gradients across the membrane, the membrane voltage and the stoichiometry (Mullins, 1979; Blaustein & Lederer, 1999). ATP is not an energy source for NCX but it is an intracellular activator possibly via phospholipid metabolism (Hilgemann & Ball, 1996).

Initially, Mullins (1979) proposed a 4:1 stoichiometry of NCX based on thermodynamic grounds. However, in cardiac myocytes the stoichiometry has been considered to be 3:1 based on measurements of ion fluxes (Pitts, 1979; Wakabayashi & Goshima, 1981; Reeves & Hale, 1984), $[Na^+]_i$ and/or $[Ca^{2+}]_i$ (Axelsen & Bridge, 1985; Sheu & Fozzard, 1985; Crespo *et al.* 1990) and the reversal potential of I_{NCX} (E_{NCX}) (Kimura *et al.* 1986, 1987; Ehara *et al.* 1989; Yasui & Kimura, 1990). However, recently Fujioka *et al.* (2000) reported that the stoichiometry of NCX in guinea-pig ventricular cells was 4:1 or variable from measurements of E_{NCX} with the inside-out 'macropatch' method, thus challenging the stoichiometry of 3:1. More recently, with whole-cell voltage-clamp, Dong *et al.* (2002) also reported 4:1 stoichiometry of NCX1.1 expressed in HEK cells. Therefore, we re-examined the stoichiometry of NCX in guinea-pig cardiac ventricular myocytes by simultaneously measuring E_{NCX} and $[Ca^{2+}]_i$ with the whole-cell voltage-clamp and confocal microscopy, respectively.

Our preliminary data were presented at the Cellular and Molecular Physiology of Sodium–Calcium Exchange meeting of the 2001 American Physiological Society as an abstract (Hinata *et al.* 2001).

METHODS

Isolation of cells

All experiments were performed in accordance with the regulations of the Animal Research Committee of Fukushima Medical University. Male guinea-pigs weighing 250–400 g were anaesthetized by intraperitoneal injection of 250 mg kg^{-1} sodium pentobarbital with 2.5 U g^{-1} heparin. The chest was opened under artificial ventilation, the aorta was cannulated *in situ*, and the heart was removed. After washing out the blood with Tyrode

solution, the heart was mounted in a Langendorff perfusion system. The perfusate was changed to Ca^{2+}-free Tyrode solution to stop the heartbeat and then to one containing 0.01 % (w/v) collagenase (Wako, Osaka, Japan) and 0.002 % (w/v) alkaline protease (Nagase, Tokyo, Japan). After about 20 min, the collagenase was washed out by perfusing a high K^+, low Cl^- solution (modified KB solution; Isenberg & Klöckner, 1982). Cardiac ventricular tissue was cut into pieces in the modified KB solution and shaken to isolate the cells. The cell suspension was stored at 4 °C and the myocytes were used for the experiment within 8 h. The temperature of the bath solution was maintained at 36 ± 0.5 °C with a water jacket. Tyrode solution contained (mM): NaCl 140, KCl 5.4, $CaCl_2$ 1.8, $MgCl_2$ 1, NaH_2PO_4 0.33, glucose 5.5 and Hepes (4, (2-hydroxyethyl)-1-piperazine-ethanesulfonic acid)-NaOH 5 (pH 7.4). The modified KB solution contained (mM): KOH 70, L-glutamic acid 50, KCl 40, taurine 20, KH_2PO_4 20, $MgCl_2$ 3, glucose 10, EGTA 0.2 and Hepes-KOH 10 (pH 7.2).

Patch-clamp recording

Membrane currents were recorded by the whole-cell patch-clamp method using pCLAMP7 software (Axon Instruments, Foster City, CA, USA). Single cardiac ventricular cells were placed in a recording chamber (1 ml volume) attached to an inverted microscope (Nikon, Tokyo, Japan) and were superfused with the Tyrode solution at a rate of 5 ml min^{-1}. Patch pipettes were forged from 1.3 mm diameter glass capillaries (Nihon Rikagaku Kikai, Tokyo) with a two-stage microelectrode puller (pp-83, Narishige, Tokyo, Japan). The pipette resistance was 3–5 MΩ when filled with the pipette solution. The composition of the pipette solution was (mM): NaCl 20, BAPTA (1,2-bis (2-aminophenoxy)-ethane-N,N,N′,N′-tetraacetic acid) 20, $CaCl_2$ 9, 9.5 or 10 (calculated free Ca^{2+} concentrations, 184, 200 or 226 nM, respectively), CsOH 120, aspartic acid 50, $MgCl_2$ 3, MgATP 5 and Hepes 20 (pH 7.2 with aspartic acid). In some experiments, 10 mM instead of 9 mM $CaCl_2$ was used in the pipette solution. Calculated E_{NCX} at 9 and 10 mM added Ca^{2+} were respectively −73 and −68 mV at 3:1, and −11 and −8 mV at 4:1. Since the results at 10 mM were similar to those with 9 mM $CaCl_2$, the data were included. The extracellular solution contained (mM): NaCl 140, $CaCl_2$ 1, $MgCl_2$ 1, ouabain 0.02, nifedipine or D600 0.01, ryanodine 0.01 and Hepes-NaOH 5 (pH 7.2). Nifedipine and D600 were used to block Ca^{2+} channels and neither drug affected I_{NCX}. The electrode was connected to a patch-clamp amplifier (CEZ-2300, Nihon Kohden, Tokyo, Japan). Recording signals were filtered at 2.5 kHz bandwidth, and the series resistance was compensated.

Ramp pulses of 500 ms duration were given with 10 s intervals in the experiments shown in Figs 1 and 2 and with 3 s intervals in the experiment shown in Figs 4 and 5. The ramp pulse was initially depolarized from a holding potential of −60 to +20 mV, then hyperpolarized to −100 mV and depolarized back to the holding potential at a speed of 680 mV s^{-1}. The stoichiometry was determined by an equilibrium potential of NCX (E_{NCX}), which is given by the following equation: $E_{NCX} = (nE_{Na} - E_{Ca})/(n - 2)$ where n is a stoichiometry of Na^+, and E_{Na} and E_{Ca} are equilibrium potentials of Na^+ and Ca^{2+}, respectively. The descending limb of the ramp was used to plot I–V curves without capacitative current compensation. Ca^{2+} current, K^+ currents, Na^+–K^+ pump current and Ca^{2+} release channels of the sarcoplasmic reticulum were blocked by nifedipine or D600, Cs^+, ouabain and ryanodine in the external solution, respectively.

Measurement of $[Ca^{2+}]_i$

The whole-cell voltage-clamp was performed using a CEZ-2400 amplifier (Nihon Kohden, Tokyo, Japan). Two-dimensional Ca^{2+} images were obtained by a fast scanning confocal fluorescent microscopy (Nikon RCM-8000; Nikon, Tokyo, Japan) equipped with a Fluor 40 × 1.15 NA, water immersion objective lens (Nikon, Tokyo, Japan) and Ratio3 software (Nikon, Tokyo, Japan). Recordings were started at least 5 min after rupturing the patch membrane to allow 100 μM indo-1 (Dojin, Kumamoto, Japan) to diffuse into the cell from the pipette. The excitation wavelength from an argon ion laser was 351 nm and the emission wavelengths were 405 and 485 nm. The resolution of the microscopy was approximately 0.4 μm × 0.3 μm × 1.5 μm (x, y and z) by the measurement using fluorescent beads. The Ca^{2+} image was scanned over a full frame (512 pixels × 512 pixels; 170 μm × 140 μm). Calibration of the indo-1 signal was performed *in vitro* using the pipette solution containing 20 mM BAPTA with various concentrations of added Ca^{2+}. The following equation was used : $[Ca^{2+}]_i = K_d(R_{min} - R)/(R - R_{max})$, where K_d is the dissociation constant of indo-1 (217 nM), R is the fluorescence ratio and R_{min} and R_{max} are the fluorescence ratios in the absence of and with saturation of Ca^{2+}, respectively (Dissociation Constant Calculator; Molecular Probes, Eugene, USA).

In vivo calibration of indo-1 would be better than *in vitro* calibration, because the K_d value of indo-1 has been reported to be higher *in vivo* than *in vitro* (Negulescu & Machen, 1990; Harkins *et al.* 1993; Kawanishi *et al.* 1994; Bassani *et al.* 1995). However, *in vivo* calibrations reported were in general performed with acetoxymethyl (AM) form of indo-1 in intact cells where the cell interior was not dialysed with a pipette solution containing a high concentration of calcium chelator such as BAPTA. In the present study, the cell was dialysed with a pipette solution containing indo-1 and 20 mM BAPTA, and this might have made *in vivo* K_d value of indo-1 similar to the *in vitro* value. Therefore we used *in vitro* calibration of indo-1 for $[Ca^{2+}]_i$. All the recordings were carried out at 36 ± 1 °C.

Data analysis

All the values are presented as means ± S.E.M. (number of experiments). Student's t test and analysis of variance were used for the statistical analyses. P values of less than 0.05 were considered to be significant.

RESULTS

Measurement of E_{NCX} by changing $[Ca^{2+}]_o$ at different holding potentials

To determine the stoichiometry of NCX, we measured E_{NCX} by a brief application of 1 mM Ni^{2+}, a selective NCX inhibitor, to the external solution. The holding potential (HP) was set at −73 mV which was the predicted E_{NCX} value for a 3:1 stoichiometry at 140 mM $[Na^+]_o$, 1 mM $[Ca^{2+}]_o$, 20 mM $[Na^+]_i$, 184 nM $[Ca^{2+}]_i$. Figure 1*A* shows concatenated current responses to ramp voltage pulses given every 10 s at −73 mV HP. Pulse intervals were omitted from the figure to clearly demonstrate the holding current level. $[Ca^{2+}]_o$ was initially at 1 mM and was raised to 2 mM. Ni^{2+} (1 mM) was added briefly to the external solution to block I_{NCX} in order to measure E_{NCX} at each $[Ca^{2+}]_o$. Figure 1*B* and *C* illustrate the current–voltage (I–V) relation curves of the control (a, c) and in the presence of 1 mM Ni^{2+} (b, d) at 1 and 2 mM $[Ca^{2+}]_o$, respectively. Figure 1*D* shows difference I–V curves of the Ni^{2+}-sensitive currents from Fig. 1*B* (a − b) and Fig. 1*C*

Table 1. Summarized results of experiments represented in Figs 1 and 2

	HP (mV)	E_{NCX} (mV)	$[Ca^{2+}]_o$ 1→0.5 mM ΔE_{NCX} (mV)	$[Ca^{2+}]_o$ 1→2 mM ΔE_{NCX} (mV)	$[Na^+]_o$ 140 →200 mM ΔE_{NCX} (mV)
Experimental values	−11	−15 ± 1 (15)	4 ± 1 (5)	−5 ± 1 (5)	8 ± 1 (5)
	−42	−47 ± 1 (14)	9 ± 1 (5)	−5 ± 1 (5)	14 ± 1 (6)
	−73	−69 ± 2 (11)	6 ± 2 (5)	−10 ± 2 (5)	22 ± 1 (5)
	Stoichiometry				
Theoretical values	4 : 1	−11	9	−9	18
	3 : 1	−73	18	−18	29

HP, holding potential; E_{NCX}, reversal potential of I_{NCX} (E_{NCX} values are control values at 1 mM $[Ca^{2+}]_o$ and $[Na^+]_o$); ΔE_{NCX}, shift in E_{NCX}. Experimental values of E_{NCX} and ΔE_{NCX} are means ± S.E.M. (number of cells).

(c − d). E_{NCX} of (a − b) was −70 mV and E_{NCX} of (c − d) was −76 mV. Therefore, E_{NCX} was shifted by −6 mV upon changing $[Ca^{2+}]_o$ from 1 to 2 mM at −73 mV HP, which was smaller than the theoretical value (−18 mV) at a 3:1 but close to that (−9 mV) at a 4:1 stoichiometry.

Using the same protocol, we measured E_{NCX} and shifts of E_{NCX} (ΔE_{NCX}) at two other HPs: −11 mV, a theoretical E_{NCX} at a 4:1 stoichiometry (Fig. 1*F*) and −42 mV (Fig. 1*E*) which is the middle value between −11 and −73 mV. In addition, $[Ca^{2+}]_o$ was lowered from 1 to 0.5 mM at each HP (figures not shown) and ΔE_{NCX} were evaluated. The results are summarized in Table 1.

We tested whether the currents measured were purely due to NCX operation, and were not contaminated by other currents through, for example, Ca^{2+}-activated non-selective cation channels, stretch-operated cation channels, Ca^{2+}-activated Cl^- channels or incompletely inactivating Na^+ channels. At −11 mV HP, 20 μM tetrodotoxin (TTX) and 100 μM niflumic acid did not affect the current, indicating that incompletely inactivating Na^+ current and Cl^- currents were not contaminated. Gadolinium at 100 μM inhibited the current with a reversal potential near −11 mV HP, which was almost identical to that inhibited by subsequently added KB-R7943, confirming that

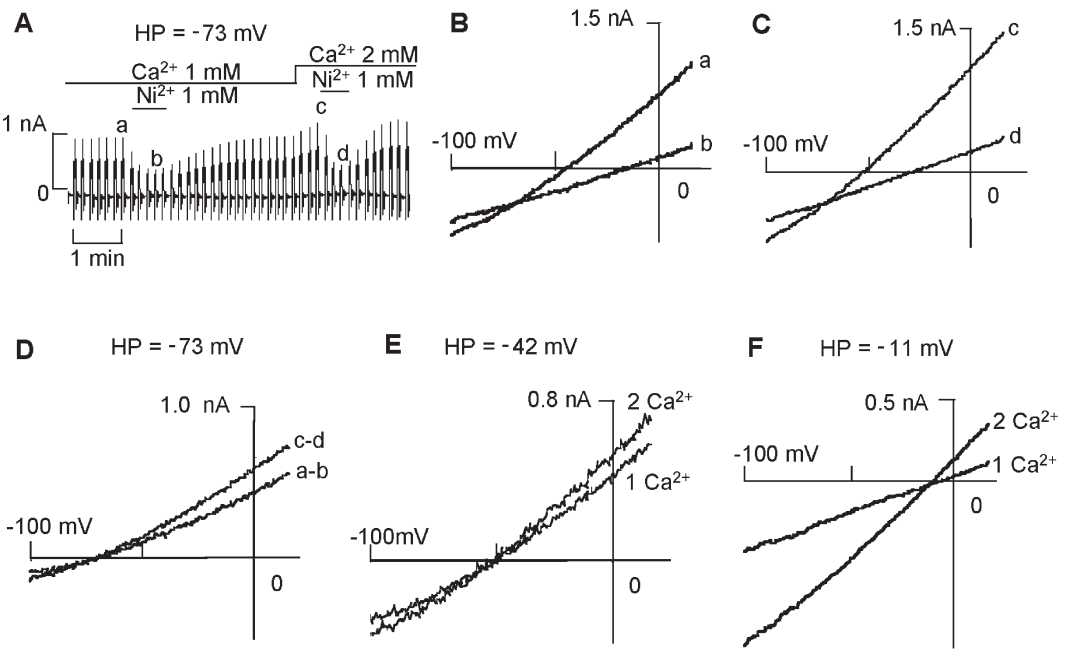

Figure 1. E_{NCX} at 1 and 2 mM $[Ca^{2+}]_o$ at three different HPs

A, concatenated current responses without pulse intervals. $[Ca^{2+}]_o$ was raised from 1 to 2 mM at −73 mV HP. Ni^{2+} was applied to block I_{NCX} and detect E_{NCX} at each $[Ca^{2+}]_o$. *B*, *I–V* curves of control (a) and in the presence of Ni^{2+} (b) at 1 mM $[Ca^{2+}]_o$ obtained from *A*. *C*, *I–V* curves of control (c) and in the presence of Ni^{2+} (d) at 2 mM $[Ca^{2+}]_o$ obtained from *A*. *D*, *I–V* curves of net Ni^{2+}-sensitive currents obtained by subtraction from *B* (a − b) and *C* (c − d). *E*, *I–V* curves of net Ni^{2+}-sensitive currents obtained by subtraction at 1 and 2 mM $[Ca^{2+}]_o$ at −42 mV HP. *F*, *I–V* curves of net Ni^{2+}-sensitive currents at 1 and 2 mM $[Ca^{2+}]_o$ at −11 mV HP.

gadolinium inhibited I_{NCX} (Zhang & Hancox, 2000) and that the stretch-operated cation current was not involved. KB-7943 and Ni^{2+} inhibited currents with similar reversal potentials near −11 mV HP, indicating that the involvement of non-selective cation current was unlikely, because KB-R7943 does not inhibit a Ca^{2+}-activated non-selective cation current (unpublished data).

As seen in Table 1, the measured E_{NCX} values were different at three different HPs, even though the ionic conditions were the same. E_{NCX} almost coincided with each HP. The values of ΔE_{NCX} were smaller than expected at stoichiometries of 3:1 and 4:1 with each intervention at almost all HPs, although some values are close to those expected at a stoichiometry of 4:1. These results suggested that $[Ca^{2+}]_i$ and/or $[Na^+]_i$ were altered by I_{NCX} flow.

Measurement of E_{NCX} by changing $[Na^+]_o$

Since changing $[Ca^{2+}]_o$ appeared to change $[Ca^{2+}]_i$ and/or $[Na^+]_i$, we next measured ΔE_{NCX} upon changing $[Na^+]_o$, because changing $[Na^+]_o$ might affect $[Ca^{2+}]_i$ and/or $[Na^+]_i$ less dramatically. A representative concatenated current response is shown in Fig. 2*A*. Currents during the pulse intervals were omitted in Fig. 2*A*. The protocol was the same as that for Fig. 1. Figure 2*B* and *C* illustrate *I–V* curves of the control (a, c) and in the presence of 1 mM Ni^{2+} (b, d) at 140 and 200 mM $[Na^+]_o$, respectively, at −73 mV HP. Figure 1*D* shows difference *I–V* curves of the Ni^{2+}-sensitive currents from Fig. 2*B* (a − b) at 140 mM $[Na^+]_o$ and from Fig. 2*C* (c − d) at 200 mM $[Na^+]_i$. E_{NCX} of (a − b) was −70 mV and E_{NCX} of (c − d) was −50 mV. ΔE_{NCX} was 22 ± 1 mV ($n = 5$) upon changing $[Na^+]_o$ from 140 to 200 mM at −73 mV HP. We performed this experiment at the two other HPs and the results are presented in Table 1. ΔE_{NCX} was smaller as HPs were less negative. ΔE_{NCX} was close to that expected at 4:1 at −42 and −73 mV HP but was significantly smaller at −11 mV than that expected at 4:1 and 3:1. This result indicated that changing $[Na^+]_o$ also changed $[Ca^{2+}]_i$ and/or $[Na^+]_i$.

Measurement of $[Ca^{2+}]_i$

In the above experiments, ΔE_{NCX} was sometimes close to that expected at a stoichiometry of 4:1, but other times it was significantly smaller than that expected at a stoichiometry of 4:1, which was even further smaller than that expected at a stoichiometry of 3:1. In addition, E_{NCX} depended on HP. These results suggested that intracellular ion concentrations, especially $[Ca^{2+}]_i$, were changed by I_{NCX} flow because $[Na^+]_i$ was more diffusible than $[Ca^{2+}]_i$ in the cell, especially in the presence of BAPTA. Therefore, we measured $[Ca^{2+}]_i$ and E_{NCX} simultaneously with 100 μM indo-1 in the pipette solution using confocal fluorescent microscopy under the whole-cell voltage-clamp. Representative images of the same cell at two different HPs are shown in Fig. 3. Ionic conditions were the same as those at 1 mM $[Ca^{2+}]_o$ and 140 mM $[Na^+]_o$ in Figs 1 and 2. Initially HP was at −11 mV (Fig. 3*A*) and then it was changed to −73 mV (Fig. 3*B*) in this cell and the reverse

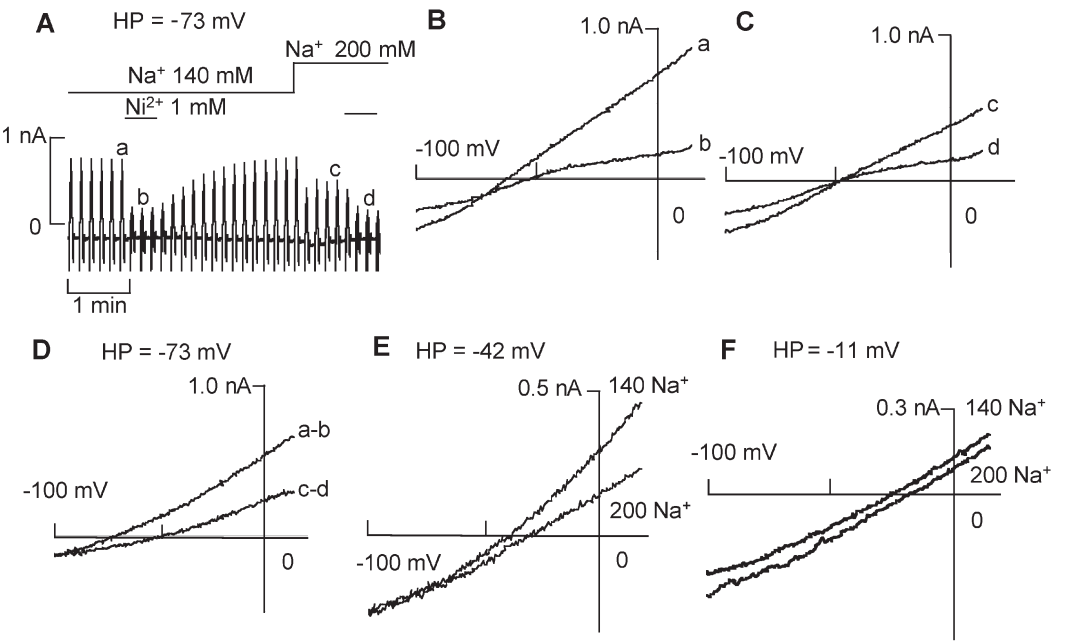

Figure 2. Effect of raising $[Na^+]_o$ on E_{NCX} at three different HPs

A, concatenated current responses without pulse intervals. $[Na^+]_o$ was raised from 140 to 200 mM at −73 mV HP. *B*, *I–V* curves of control (a) and in the presence of Ni^{2+} (b) at 140 mM $[Na^+]_o$. *C*, *I–V* curves of control (c) and in the presence of Ni^{2+} (d) at 200 mM $[Ca^{2+}]_o$. *D*, *I–V* curves of net Ni^{2+}-sensitive currents obtained by subtraction from *B* (a − b) and *C* (c − d). *E*, subtracted *I–V* curves of Ni^{2+}-sensitive currents at 140 and 200 mM $[Na^+]_o$ at −42 mV HP. *F*, subtracted *I–V* curves of Ni^{2+}-sensitive currents at 140 and 200 mM $[Na^+]_o$ at −11 mV HP.

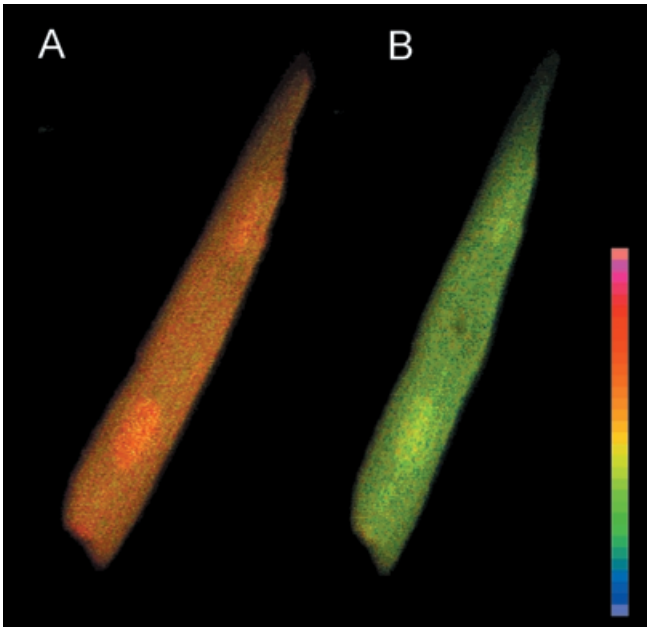

Figure 3. $[Ca^{2+}]_i$ measurement with indo-1 at two different HPs

$[Ca^{2+}]_i$ was measured using a confocal microscopy with 100 μM indo-1 in the pipette under the voltage-clamp. *A*, at −11 mV HP, $[Ca^{2+}]_i$ was 374 ± 38 nM (n = 16) (left). *B*, in the same cell at −73 mV HP, $[Ca^{2+}]_i$ was 173 ± 11 nM (n = 13). ($P < 0.0002$ by Student's t test).

order of HPs was also tested. Recordings were continued for at least 5 min after rupturing the patch membrane or after changing the membrane potential. At −11 mV HP, $[Ca^{2+}]_i$ was 374 ± 38 nM (n = 16) (Fig. 3*A*) and E_{NCX} was −13 ± 1 mV (n = 5). In contrast, in the same cell at −73 mV HP, $[Ca^{2+}]_i$ was 173 ± 11 nM (n = 13) and E_{NCX} was −70 ± 1 mV (n = 5). The predicted $[Ca^{2+}]_i$ was 184 nM at −73 and −11 mV at stoichiometries of 3:1 and 4:1, respectively. The $[Ca^{2+}]_i$ of 173 ± 11 nM at −73 mV HP was close to the predicted value at a stoichiometry of 3:1, while 374 ± 38 nM at −11 mV was too high for a 4:1 stoichiometry. Thus, the results of $[Ca^{2+}]_i$ measurements supported a 3:1 stoichiometry.

Measurement of E_{NCX} during the recovery from Ni^{2+}-inhibition

Since $[Ca^{2+}]_i$ was in accordance with a 3:1 stoichiometry, we attempted to measure E_{NCX} again by the whole-cell clamp with a protocol which would minimize ionic concentration change due to I_{NCX} flow. We inhibited I_{NCX} completely with 5 mM Ni^{2+} at the onset of the whole-cell clamp and examined E_{NCX} during the recovery of I_{NCX} after washing out Ni^{2+} (Fig. 4). We at first performed the experiment using the same ionic conditions used in Fig. 1 at −73 and −11 mV HP. However the difference in the reversal potential was not clear between the two HPs. Therefore we employed an external solution containing higher concentrations of 200 mM $[Na^+]_o$ and 9 mM $[Ca^{2+}]_o$ and a pipette solution containing 20 mM Na^+ and 200 nM free Ca^{2+} (20 mM BAPTA and 9.5 mM Ca^{2+}). The external solution is hyperosmotic and may modulate the magnitude of I_{NCX}, but does not affect E_{NCX} (Wright *et al.* 1995). The predicted E_{NCX} was −100 mV at a 3:1 stoichiometry and −20 mV at a 4:1 stoichiometry. Representative concatenated current responses at −90 mV HP are shown in Fig. 4*A* and at −20 mV HP in Fig. 4*B*.

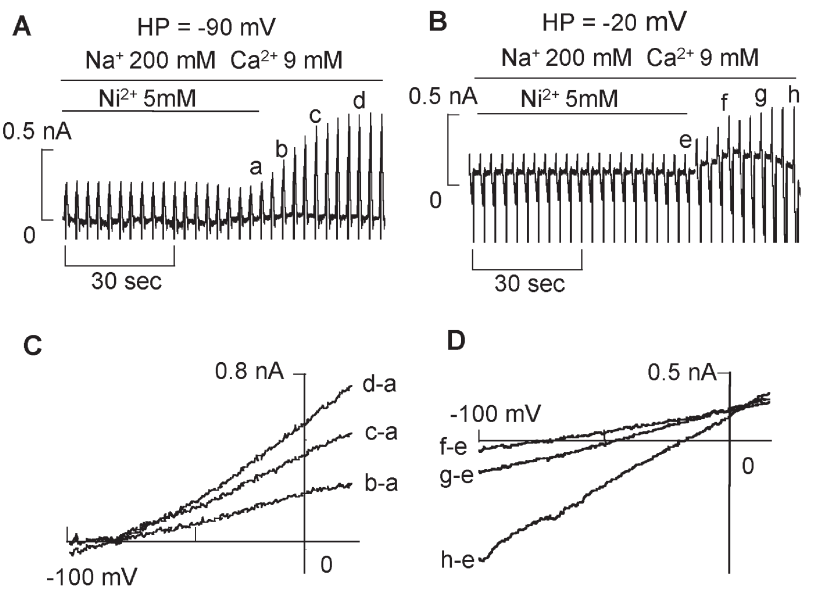

Figure 4. Effects of −90 mV HP (E_{NCX} at a 3:1 stoichiometry) and −20 mV HP (E_{NCX} at a 4:1 stoichiometry) on E_{NCX} during the recovery from Ni^{2+} inhibition

A, concatenated current responses at −90 mV HP. *B*, concatenated current responses at −20 mV HP. *C*, difference *I–V* curves of the corresponding labels from *A*. E_{NCX} were around −90 mV and did not dramatically change with time. *D*, difference *I–V* curves of the corresponding labels from *B*. E_{NCX} was initially at about −70 mV and shifted toward −20 mV HP with time.

Table 2. Summarized results of experiments represented in Fig. 4

HP (mV)	Initial E_{NCX} (mV)	Steady state E_{NCX} (mV)
−20	−56 ± 4 (6)	−22 ± 2 (6)
−90	−80 ± 2 (6)	−84 ± 4 (6)

E_{NCX} values are means ± S.E.M. (number of cells).

Table 3. Summarized results of experiments represented in Fig. 5

HP (mV)	Initial E_{NCX} (mV)	Steady state E_{NCX} (mV)
−20	−22 ± 2 (5)	−25 ± 4 (5)
−90	−19 ± 4 (7)	−32 ± 10 (7)

E_{NCX} values are means ± S.E.M. (number of cells).

Ramp pulse interval was 3 s instead of 10 s. Ni^{2+} at 5 mM was added to the external solution at the beginning of the whole-cell clamp and was washed out after about 5 min. Figure 4*C* shows the difference *I–V* curves at −90 mV HP. E_{NCX} developed at around −90 mV and did not change with time. In contrast, at −20 mV HP, E_{NCX} of the difference *I–V* curves appeared initially at around −70 mV and shifted toward −20 mV with time (Fig. 4*D*). As shown in Table 2, the average steady state values coincided with a 3:1 stoichiometry but not with a 4:1 stoichiometry.

To further confirm our results, we performed the above protocol under the ionic conditions where a theoretical E_{NCX} was approximately −20 mV at a 3:1 stoichiometry. With 200 mM $[Na^+]_o$, 0.5 mM $[Ca^{2+}]_o$, 20 mM $[Na^+]_i$ and 226 nM $[Ca^{2+}]_i$, E_{NCX} calculated is −21 mV at a 3:1 stoichiometry. Figure 5*A* shows representative concatenated currents recorded at −20 mV HP. Figure 5*C* shows the difference *I–V* curves obtained by subtraction as labelled. E_{NCX} developed initially near the holding potential of −22 ± 2 mV ($n = 5$) and did not shift with time. Steady state E_{NCX} after about 36 s was −25 ± 2 mV ($n = 5$) (Table 3). This result also supports a 3:1 stoichiometry. In contrast, under the same ionic conditions, when HP was held at −90 mV, a significantly more negative HP than E_{NCX} at a 3:1 stoichiometry, E_{NCX} developed initially at −19 ± 4 mV ($n = 5$) and shifted to a steady state E_{NCX} of −32 ± 10 mV ($n = 5$) after 36 s. Thus when HP was away from expected E_{NCX}, the initial E_{NCX} soon after washing out Ni^{2+} coincided with the value expected for a 3:1 stoichiometry but then shifted with time. These data strongly support that the stoichiometry of NCX is 3:1 rather than 4:1.

DISCUSSION

When we measured E_{NCX} at three different HPs, −11, −42 and −73 mV, E_{NCX} almost coincided with HP even though the compositions of the external and pipette solutions were identical. Furthermore, when we measured the E_{NCX} shifts (ΔE_{NCX}) by changing $[Ca^{2+}]_o$ or $[Na^+]_o$, ΔE_{NCX} values were closer to that expected at a 4:1 stoichiometry than 3:1 or most often smaller than those expected for both 4:1 and 3:1 stoichiometries at any of the HPs. The most likely cause of the smaller ΔE_{NCX} upon changing $[Ca^{2+}]_o$ and $[Na^+]_o$ was that Ca^{2+} and/or Na^+ accumulated (or depleted) under the membrane because I_{NCX} approached NCX equilibrium at a given holding potential. In addition, 1 mM Ni^{2+} did not inhibit I_{NCX} completely and thus I_{NCX} flow during Ni^{2+} inhibition allowed $[Ca^{2+}]_i$ and/or $[Na^+]_i$ change. Contamination of other currents such as non-inactivating Na^+ current and Cl^- currents could be denied, because 20 μM tetrodotoxin (TTX) and 100 μM niflumic acid did not affect the current at −11 and −73 mV HP. Gadolinium at 100 μM inhibited the current with the reversal potential near −11 mV HP, which was identical to that inhibited

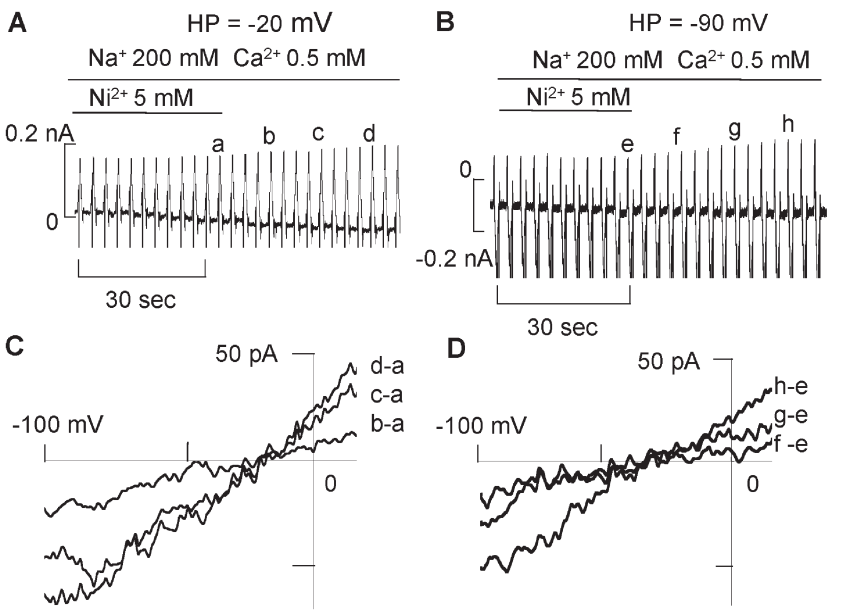

Figure 5. Effects of −20 mV HP (E_{NCX} at a 3:1 stoichiometry) and −90 mV HPs on E_{NCX} during the recovery of I_{NCX} from Ni^{2+} inhibition

A, concatenated currents at −20 mM HP which is E_{NCX} at a 3:1 stoichiometry. *B*, concatenated currents at −90 mV HP which is a more negative voltage than E_{NCX} at a 3:1 stoichiometry. *C*, difference *I–V* curves of the corresponding labels from *A*. E_{NCX} was at about −20 mV and did not shift with time. *D*, difference *I–V* curves of the corresponding labels from *B*. E_{NCX} developed initially at around −20 mV and then shifted toward −34 mV with time.

further by subsequently added KB-R7943. This confirmed that gadolinium inhibited I_{NCX} (Zhang & Hancox, 2000) and that a stretch-activated cation current was not involved. Contamination of Ca^{2+}-activated nonselective cation current was also negated because KB-R7943- and Ni^+-inhibited currents had similar reversal potentials while KB-R7943 does not inhibit the Ca^{2+}-activated cation current (unpublished data).

The fact that E_{NCX} tended to coincide with a holding potential at any ionic concentration indicates that the method we employed in Figs 1 and 2 for measuring E_{NCX} to determine the stoichiometry had serious limitations. To overcome this difficulty, we measured $[Ca^{2+}]_i$ with indo-1 fluorescence using confocal microscopy under the voltage-clamp. $[Ca^{2+}]_i$ at −73 mV HP, or E_{NCX} at a 3:1 stoichiometry, was 173 ± 11 nM (n = 13). Thus the value was almost consistent with the theoretical $[Ca^{2+}]_i$ of 184 nM. However, under the same ionic conditions, $[Ca^{2+}]_i$ at −11 mV HP, or E_{NCX} at a 4:1 stoichiometry, was 374 ± 38 nM (n = 16). This value was significantly higher than the theoretical value of 184 nM. In addition, in spite of using the same cell, $[Ca^{2+}]_i$ were significantly changed between the two different HPs. This was a surprising result because $[Ca^{2+}]_i$ accumulated even in the presence of 20 mM BAPTA. Thus, the $[Ca^{2+}]_i$ measurement supported a 3:1 but not a 4:1 stoichiometry.

We performed the whole-cell voltage-clamp experiment again and examined E_{NCX} with a different protocol, as shown in Figs 4 and 5. We initially inhibited I_{NCX} almost completely with 5 mM Ni^{2+} instead of 1 mM Ni^{2+}, and then washed out Ni^{2+} to measure E_{NCX} during the recovery of I_{NCX} from Ni^{2+} inhibition. When the HP was at E_{NCX} for a 3:1 stoichiometry, the E_{NCX} developed initially near the theoretical value for a 3:1 stoichiometry and did not change with time (Fig. 4*A* and *C*, Fig. 5*A* and *C*). In contrast, when the HP was at the theoretical E_{NCX} for a 4:1 stoichiometry, which was more positive than a 3:1 E_{NCX} (Fig. 4*B* and *D*), or when the HP was significantly more negative than a 3:1 E_{NCX} (Fig. 5*B* and *D*), I_{NCX} developed initially with E_{NCX} closed to that expected for a 3:1 stoichiometry and then shifted with time toward each HP (Tables 2 and 3). These results also support a 3:1 stoichiometry.

We learned from this study that it is rather difficult to control $[Ca^{2+}]_i$ even with 20 mM BAPTA in the pipette solution under the whole-cell voltage-clamp when I_{NCX} flowed. In other words, NCX has a strong tendency to approach its equilibrium at a holding potential by changing $[Ca^{2+}]_i$ and/or $[Na^+]_i$, and this is why E_{NCX} tends to coincide with a given holding potential at a steady state. Recently, using the whole-cell voltage-clamp, Dong *et al.* (2002) reported 4:1 stoichiometry by measuring E_{NCX} of NCX1.1 overexpressed in HEK cells. Although their data of E_{NCX} fitted to theoretically expected 4:1 stoichiometry, they used a fixed holding potential of 0 mV with a rather low concentration of 10 mM EGTA or BAPTA in the pipette solution and therefore there is a possibility that E_{NCX} they measured were shifted to the holding potential of 0 mV, and thus apparently fitted to 4:1 rather than 3:1 stoichiometry. This possibility is also discussed for the macro-patch data in the following.

Fujioka *et al.* (2000) concluded that the stoichiometry was 4:1 or variable depending on external and cytoplasmic Ca^{2+} or Na^+ concentrations. They examined E_{NCX} with inside-out macro-patches which they estimated to be devoid of $[Ca^{2+}]_i$ accumulation. However, based on our present results we suspect that $[Ca^{2+}]_i$ accumulation might have occurred on the cytoplasmic side of the inside-out macro-patch membrane in their experiment for the following reasons. First, they used a rather low concentration of 10 mM EGTA as a Ca^{2+} chelator added to a high concentration of 8.79 mM $CaCl_2$ to give 1 μM free Ca^{2+} in the cytoplasmic solution. EGTA has Ca^{2+} binding kinetics slower than that of BAPTA (Tsien, 1980). Our data indicated that it was difficult to control $[Ca^{2+}]_i$ even with 20 mM BAPTA in the pipette solution. Second, they fixed the holding potential at 0 mV, which was good to avoid interference by a Ca^{2+}-activated non-selective cation current that reverses at 0 mV (Ehara *et al.* 1988), but it might have facilitated Ca^{2+} accumulation during the outward I_{NCX} flow at 0 mV. For example, under the ionic conditions of Fujioka *et al.* (2000) with 145 mM $[Na^+]_o$, 50 mM $[Na^+]_i$, 2 mM $[Ca^{2+}]_o$ and 1 μM $[Ca^{2+}]_i$, the theoretical E_{NCX} at a 3:1 stoichiometry was −117 mV, while the E_{NCX} they measured was around −50 mV, which they interpreted as an E_{NCX} at a 4:1 stoichiometry. However, this may have been due to $[Ca^{2+}]_i$ accumulation rather than a 4:1 stoichiometry, because if $[Ca^{2+}]_i$ rose to 10 μM, E_{NCX} would be −56 mV at a 3:1 stoichiometry. Fujioka *et al.* (2000) demonstrated that I_{NCX} of 1.5 pA was induced by 50 mM $[Na^+]_i$ at 0 mV, which could induce Ca^{2+} influx of 5 μM s^{-1} by roughly estimating the space under the macro-patch membrane as a half sphere with 6 μm diameter and thus an increase of $[Ca^{2+}]_i$ to 10 μM might be possible due to I_{NCX} flow.

Third, the data of Fujioka *et al.* (2000) indicated that the stoichiometry was closer to 3:1 when $[Na^+]_i$ was lower (~9 mM) or $[Ca^{2+}]_i$ was higher (100 μM) at fixed concentrations of 145 mM $[Na^+]_o$ and 2 mM $[Ca^{2+}]_o$, and that the stoichiometry was 4 or more when $[Na^+]_i$ was higher (9–40 mM) or $[Ca^{2+}]_i$ was lower (0.1–10 μM). Higher $[Na^+]_i$ induced larger Ca^{2+} influx leading to Ca^{2+} accumulation on the cytoplasmic side of the membrane, especially at lower $[Ca^{2+}]_i$. This tendency was seen in both macro-patch and giant-patch data, but was more prominent in the macro-patch than the giant-patch (Fujioka *et al.* 2000). This may have led to their conclusion of a 4:1 or 5:1 stoichiometry.

Where does Ca^{2+} accumulate in the macro-patch? The macro-patch is very likely to maintain the complex structure of the cardiac surface membrane including the T-tubules (Davis *et al.* 2001), unlike the smooth giant-patch obtained from the fully extended 'bleb' membrane of the relaxed myocyte (Collins *et al.* 1992). NCX molecules are more densely localized in the transverse tubules than the surface membrane (Frank *et al.* 1992; Yang *et al.* 2002). Activity of these localized NCX may lead to Ca^{2+} accumulation in a limited space under the membrane. Accumulation effects were also seen in the giant-patch data (Fujioka *et al.* 2000), which may indicate that there may be a limited space for rapid diffusion to occur just under the NCX molecules. Although Fujioka *et al.* (2000) simulated ion flux in the inside-out patch membrane, simulated curves do not always appear to fit the experimentally obtained curve. Thus there may be a limited space immediately under the NCX molecule which prevents immediate free diffusion with the bulk solution.

We conclude that the stoichiometry of cardiac Na^+–Ca^{2+} exchange is 3:1.

REFERENCES

Axelsen, P. H. & Bridge, J. H. B. (1985). Electrochemical ion gradients and the Na/Ca exchange stoichiometry. Measurements of these gradients are thermodynamically consistent with a stoichiometric coefficient>3. *Journal of General Physiology* **85**, 471–475.

Bassani, J. W., Bassani, R. A. & Bers, D. M. (1995). Calibration of indo-1 and resting intracellular $[Ca]_i$ in intact rabbit cardiac myocytes. *Biophysical Journal* **68**, 1453–1460.

Blaunstein, M. P. & Lederer, W. J. (1999). Sodium/calcium exchange: Its physiological implications. *Physiological Reviews* **79**, 763–854.

Crespo, L. M., Grantham, C. J. & Cannnell, M. B. (1990). Kinetics, stoichiometry, role of Na^+–Ca^{2+} exchange mechanism in isolated cardiac myocytes. *Nature* **345**, 618–621.

Collins, A., Somlyo, A. V. & Hilgemann, D. W. (1992). The giant cardiac membrane patch method: stimulation of outward Na(+)–Ca^{2+} exchange current by MgATP. *Journal of Physiology* **454**, 27–57.

Davis, J. J., Hill, H. A. & Powell, T. (2001). High resolution scanning force microscopy of cardiac myocytes. *Cell Biology International* **25**, 1271–1277.

Dong, H., Dunn, J. & Lytton, J. (2002). Stoichiometry of the cardiac Na^+/Ca^{2+} exchanger NCX1.1 measured in trasnfected HEK cells. *Biophysical Journal* **82**, 1943–1952.

Ehara, T., Matsuoka, S. & Noma, A. (1989). Measurement of reversal potential of Na^+–Ca^{2+} exchange current in single guinea-pig ventricular cells. *Journal of Physiology* **410**, 227–249.

Ehara, T., Noma, A. & Ono, K. (1988). Calcium-activated non-selective cation channel in ventricular cells isolated from adult guinea-pig hearts. *Journal of Physiology* **403**, 117–133.

Frank, J. S., Mottino, G., Reid, D., Molday, R. S. & Philipson K. D. (1992). Distribution of the Na^+–Ca^{2+} exchange protein in mammalian cardiac myocytes: an immunofluorescence and immunocolloidal gold-labeling study. *Journal of Cell Biology* **117**, 337–345.

Fujioka, Y., Komeda, M. & Matsuoka, S. (2000). Stoichiometry of Na^+–Ca^{2+} exchange in inside-out patches excised from guinea-pig ventricular myocytes. *Journal of Physiology* **523**, 339–351.

Harkins, A. B., Kurebayashi, N. & Baylor, S. M. (1993). Resting myoplasmic free calcium in frog skeletal muscle fibers estimated with fluo-3. *Biophysical Journal* **65**, 865–881.

Hilgemann, D. W. & Ball, R. (1996). Regulation of cardiac Na^+, Ca^{2+} exchange K_{ATP} potassium channels by PIP2. *Science* **273**, 956–959.

Hinata, M., Li, L., Watanabe, Y., Watano, T. & Kimura, J. (2001). Re-examination of the stoichiometry of Na/Ca exchange with whole-cell clamp of guinea-pig ventricular myocytes. *The Physiologist* **44**, 234 (abstract).

Isenberg, G. & Klöckner, U. (1982). Calcium torerant ventricular myocytes prepared by preincubation in a 'KB' medium. *Pflügers Archiv* **395**, 6–18.

Kawanishi, T., Aosu, H., Kato, T., Uneyama, C., Toyoda, K., Ohata, H., Momose, K., & Takahashi, M. (1994). Ratio-imaging of calcium waves in cultured hepatocytes using rapid scanning confocal microscope and indo-1. *Bioimages* **2**, 7–14.

Khananshvili, D. (1990). Distinction between the two basic mechanisms of cation transport in the cardiac Na^+–Ca^{2+} exchange system. *Biochemistry* **29**, 2437–2442.

Kimura, J., Miyamae, S. & Noma, A. (1987). Identification of sodium–calcium exchange current in single ventricular cells of guinea-pig. *Journal of Physiology* **384**, 199–222.

Kimura, J., Noma, A. & Irisawa, H. (1986). Na–Ca exchange current in mammalian heart cells. *Nature* **319**, 596–597.

Li, J. M. & Kimura, J. (1991). Translocation mechanism of cardiac Na–Ca exchange. *Annals of the New York Academy of Sciences* **639**, 48–60.

Mullins, L. J. (1979). The generation of electric currents in cardiac fibers of Na/Ca exchange. *American Journal of Physiology* **236**, C103–110.

Negulescu, P. A. & Machen, T. E. (1990). Intracellular ion activities and membrane transport in pariental cells measured with fluorescent dyes. *Methods in Enzymology* **192**, 38–81.

Niggli, E. & Lederer, W. J. (1991). Molecular operations of the sodium–calcium exchanger revealed by conformation currents. *Nature* **349**, 621–624.

Pitts, B. J. (1979). Stoichiometry of sodium–calcium exchange in cardiac sarcolemmal vesicles. Coupling to the sodium pump. *Journal of Biological Chemistry* **254**, 6232–6235.

Reeves, J. P. & Hale, C. C. (1984). The stoichiometry of the cardiac sodium–calcium exchange system. *Journal of Biological Chemistry* **259**, 7733–7739.

Sheu, S. S. & Fozzard, H. A. (1985). Na/Ca exchange in the intact cardiac sodium–calcium exchange system. *Journal of Biological Chemistry* **259**, 7733–7739.

Tsien, R. Y. (1980). New calcium indicators and buffers with high selectivity against magnesium and protons: design, synthesis, and properties of prototype structures. *Biochemistry* **19**, 2396–2404.

Wakabayashi, S. & Goshima, K. (1981). Kinetic studies on sodium-dependent calcium uptake by myocardial cells and neuroblastoma cells in culture. *Biochimica et Biophysica Acta* **642**, 158–172.

Wright, A. R., Rees, S. A., Vandenberg, J. I., Twist, V. W. & Powell, T. (1995). Extracellular osmotic pressure modulates sodium–calcium exchange in isolated guinea-pig ventricular myocytes. *Journal of Physiology* **488**, 293–301.

Yang, Z., Pascarel, C., Steele, D. S., Komukai, K., Brette, C. H. & Orchard, C. H. (2002). Na^+–Ca^{2+} exchange activity is localized in the T-tubules of rat ventricular myocytes. *Circulation Research* **91**, 315–322.

YASUI, K. & KIMURA, J. (1990). Is potassium co-transported by the cardiac Na–Ca exchange? *Pflügers Archiv* **415**, 513–515.

ZHANG, Y. H. & HANCOX, J. C. (2000). Gadolinium inhibits Na(+)–Ca(2+) exchanger current in guinea-pig isolated ventricular myocytes. *British Journal of Pharmacology* **130**, 513–515.

Acknowledgements

We thank Dr Isao Matsuoka for his valuable discussion, and Dr Tomoyuki Ono and Ms Sanae Sato for their excellent technical assistance. This work was supported by Grants-in-Aid for Scientific Research from the Japan Society for the Promotion of Science (11357020, 13670092).

Author's present address

Y. Watanabe: Department of Pathophysiology, Basic Nursing, Hamamatsu University School of Medicine, Hamamatsu 431-3192, Japan.